RADIOMETRIC CALIBRATION AND EVALUATION OF ULTRACAM X AND XP USING PORTABLE REFLECTANCE TARGETS AND SPECTROMETER DATA. APPLICATION TO EXTRACT THEMATIC DATA FROM IMAGERY GATHERED BY THE NATIONAL PLAN OF AERIAL ORTHOPHOTOGRAPHY (PNOA)

F. Alvarez [a, *], T. Catanzarite [b], J. R. Rodríguez-Pérez [a], D. Nafría [c]

[a] Universidad de León. Campus de Ponferrada, s/n 24400. Ponferrada (Leon, Spain) (flor.alvarez, jr.rodriguez)@unileon.es
[b] Universidade de Vigo. Campus Universitario, s/n 36310 Vigo (Pontevedra, Spain). tainyct@gmail.com
[c] ITACYL. Junta de Castilla y Leon. Finca Zamadueñas. 47071 (Valladolid, Spain) nafgarda@itacyl.es

KEY WORDS: camera, radiometric, calibration, thematic, National Plan of Aerial Orthophotography (PNOA)

ABSTRACT:

Digital photogrammetric cameras obtain multispectral images with a high geometric accuracy and radiometric information which can be used for multiple purposes. The optimal use of this information requires a calibration and validation of the photogrammetric systems. Calibration is the process of defining the sensor response quantitatively to a known and controlled input signal. The objectives of this research are: (i) radiometric characterization and evaluation of the digital photogrammetric camera Ultracam X and Xp, (ii) partial radiometric calibration of the digital photogrammetric cameras Ultracam X and Ultracam Xp, (iii) determining the Ground Sampling Distance (GSD) influence in the calibration process, and (iv) determining the suitability of calibration for imagery gathered by the National Plan of Aerial Orthophotography (PNOA).
Two different data sets were used to conduct this research. Set A consisted of three images captured by the digital photogrammetric camera Ultracam X with a GSD of 7 cm in Barakaldo (Bizcaia, Spain), while Set B was gathered by the digital photogrammetric camera Ultracam Xp with a GSD of 25 cm in Cogollos (Burgos, Spain) for the National Plan of Aerial Orthophotography (PNOA). The in-situ calibration was performed by using 10 portable reflectance targets. The 1 m x 1 m targets were made of Alucobond® and coated with vinyl. The selected reflectance values were: 0%, 25%, 50%, 75% and 100%. Also two targets were manufactured for each reflectance value. The targets were placed in the calibration field before the flight, and their reflectance and radiance were measured with the spectrometer Fieldspec®3. The targets' nominal reflectance values were compared to the spectrometer values to check if there were significant differences (i.e. $p<0.05$ at $\alpha = 0.05$). The digital numbers corresponding to the targets in the image were compared to the nominal target reflectance and also to the values (radiances and reflectances) measured by the spectrometer. This procedure was used to perform the radiometric characterization and calibration. The results of Set A and set B were compared and implications of using a different GSD discussed. The suitability of this calibration process and their applicability to images gathered by the National Plan of Aerial Orthophotography (PNOA) provides practical recommendations to perform this calibration as a first step to extract thematic data from imagery from PNOA.

1. INTRODUCTION

Multispectral images obtained by digital photogrammetric cameras can potentially be used to extract qualitative and quantitative thematic information. Nevertheless, there are several weaknesses in current processes that are slowing down the use of radiometric information provided by these sensors. The optimal use of the technological progress requires the calibration and validation of the photogrammetric systems (Honkavaara, 2004). In this context, calibration is the process of defining quantitatively the response of a sensor to a controlled and known input signal (Cramer, 2007).
Flight conditions (i.e. atmospheric conditions, exposure characteristics, solar elevation), and sensor characteristics, as well as post-processing effects (calibration based on radiometric corrections) have an effect on image radiometry (Markelin et al., 2008). As a result, the same object generates different digital numbers depending on its location (in the same image and in different images). Therefore, to use this information in a quantitative approach it is necessary to perform a relative and/or absolute radiometric registration. Moreover, the optimal radiometric processing procedure depends on the final application and the technique selected to extract the information: (i) classic remote sensing (using normalized data from the image) or (i) methods using the characteristics of the anisotropic reflectance of the objects (bidirectional reflectance distribution function) (Honkavaara y Markelin, 2007). Any application related to extracting thematic information requires rigorous processing methods, which are well developed for satellite imagery and airborne sensors, but which are still in development for photogrammetric sensors. The previous issues indicate the need of developing a protocol to process the information in order to be able to use the photogrammetric data to extract thematic data by remote sensing techniques.
A comprehensive review of radiometric aspects of digital photogrammetric images and calibration experiences can be read in Honkavaara et al., (2009).
In this context the National Plan of Aerial Orthophotography (PNOA) is gathering multispectral digital imagery. The imagery gathered has a temporal resolution of two years; therefore, it is interesting to determine the possibility of calibrating radiometrically the multispectral images captured by PNOA to

* Corresponding author.

extract thematic information. Therefore the objectives if this research are: (i) radiometric characterization and evaluation of the digital photogrammetric camera Ultracam X and Xp, (ii) partial radiometric calibration of the digital photogrammetric cameras Ultracam X and Ultracam Xp, (iii) determining the GSD influence in the calibration process, and (iv) determining the suitability of the calibration for the imagery gathered by PNOA.

2. EXPERIMENTAL STUDY

2.1 Material and field work

Two different data sets of multispectral images were used to conduct this research. Set A consisted of three images captured by the digital photogrammetric camera Ultracam X with a Ground Sampling Distance (GSD) of 7 cm in Barakaldo (Bizcaia, Spain) on the 12th July 2009. The images were taken so that the geometric centre of each image was as close as possible to reflectance targets that were placed in the field. These images were originally processed to level 2 (according to the camera's technical specifications). Set B consisted of two images gathered by the digital photogrammetric camera Ultracam Xp with a GSD of 25 cm in Cogollos (Burgos, Spain) on the 10th July 2009 as part of the National Plan of Aerial Orthophotography (PNOA). The images in set B were already processed to level 3 (according to the camera's technical specifications), since it is the default processing level for the images acquired for PNOA in 2009.
The medium format multispectral output images obtained with Ultracam X and Xp had the characteristics which are shown in Table 1.

Characteristic		**Ultracam X**		**Ultracam Xp**	
Image Format (mm | pixel)	long track	67.824	3140	67.860	3770
	cross track	103.896	4810	103.860	5770
Pixel Size (µm)		21.600*21.600		18.000*18.000	
Focal Length (mm)		100.500		100.500	
Principal Point (Level 2) (mm)	X_ppa	0.000 ± 0.002		0.000 ± 0.002	
	Y_ppa	0.144 ± 0.002		0.120 ± 0.002	
Spectral sensitivity (nm) (min-max values)		Blue (B): 400-600, Green (G):480-660; Red (R): 580-720, Near Infrared (NIR): 620-100			

Table 1. Main characteristics of medium format multispectral output images obtained with Ultracam X and Xp, as outlined in the calibration reports.

The in-situ calibration was performed by using 10 portable reflectance targets. The 1 m x 1 m targets were made of Alucobond® and coated with vinyl. The selected nominal reflectance values were: 100% (BL), 75% (GR25), 50% (GR50), 25% (GR75) and 0% (NG). Also two targets were manufactured for each reflectance value. The targets were placed in the corresponding calibration field before the flights, and the GPS coordinates of the exterior corners were measured using a 24-channel dual-frequency RTK GPS receiver Trimble 5700, with a precision of 5 mm in static surveying mode. The data was post-processed using reference stations in order to refer the coordinates to ETRS 89.
Each set of targets with the same nominal reflectance were placed together in an increasing order of reflectance, as showed in Figure 1. Radiance and reflectance were measured for each target with the spectrometer Fieldspec®3 immediately before the flight in Barakaldo and immediately after the flight in Cogollos. The radiance was also measured immediately after the flight in both locations.
The spectrometer ASD Fieldspec®3 had a spectral range from 350 nm to 2500 nm, using a 512 element Si photodiode array for the 350-1000 nm interval, and two InGaAs photodiodes for the 1000-2500 nm range. In every case the spectrometer was calibrated before taking the measurements.

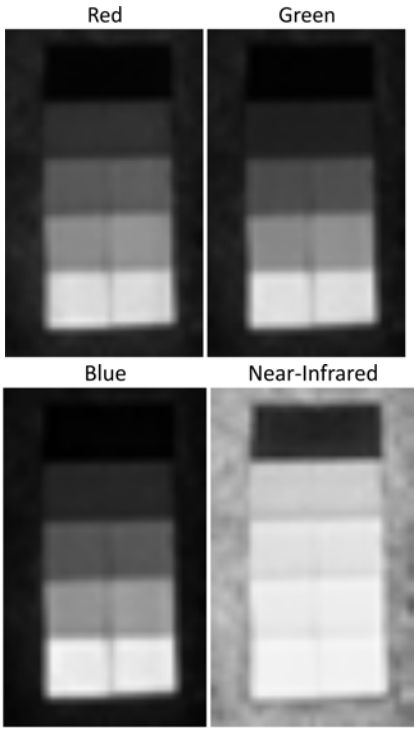

Figure 1. Portable reflectance targets (0%, 25%, 50%, 75% and 100% nominal reflectance) placed in the field (orthophoto 7017)

2.2 Methods

2.1.1. Imagery data pre-processing: images from both set A and set B were orthorectified using the Integrated Sensor Orientation (ISO) technique. The digital numbers (DNs) in each one of the spectral bands were resampled using the nearest neighbour method, so that the original DNs were not modified. Three independent orthophotos were obtained for Barakaldo (7016, 7017, 7018), while for Cogollos only one orthophoto was generated. In both cases a test was conducted to check whether the differences between the target DNs in the orthophotos and the target DNs in the original images were significantly different (i.e. $p<0.05$ at $\alpha = 0.05$). Therefore the analyses were conducted using the orthophotos, in order to be able to perform comparisons among them. The reflectance targets overlapped in three orthophotos from Barakaldo, so the same point data set was used to extract the DNs corresponding to each reflectance target for each spectral band. An analogous process was conducted for the orthophoto from Cogollos. The DNs database was filtered and the outliers were detected and removed.

2.1.2. Imagery data processing: the normality of the DN distributions were tested using the Kolmogorov-Smirnov (K-S) test at a significance level of 5% ($\alpha = 0.05$), in order to determine whether parametric or non parametric tests/statistics should be used in the data analysis. The DN statistics were

calculated for each reflectance target (mean, median, minimum, maximum, standard deviation (SD)) and for each orthophotograph.

The distribution of DNs for each pair of targets with the same nominal reflectance (BL_1 and BL_2, GR25_1 and GR25_2, GR50_1 and GR50_2, GR75_1 and GR75_2, and NG_1 and NG_2) were compared to determine if the spectral response registered by the sensor was different or whether both samples came from the same population. Thus, the non-parametric Mann–Whitney U test for independent samples was conducted at a significance level of 5% ($\alpha = 0.05$).

The DN values registered for each reflectance target were compared among the three orthophotos that were available for the Barakaldo site (e.g. DNs for BL_1 in orthophotos 7016, 7017 and 7018). The Friedman test and the Wilkoxon signed-rank test for related samples were used to check if the differences between the DNs in the different images for each reflectance target were significant. Both tests are non-parametric and suitable for continuous data; the main difference is that the first one is suitable for multiple samples (more than two), while the latter only works with two samples. In this case there are three images, so the Friedman test was performed. Since the Friedman test did not provide information about which of the samples are different (in case they are different), the Wilkoxon signed-rank test was required to identify the different samples. Both tests were conducted with a 5% ($\alpha = 0.05$) level of significance.

2.1.3. Spectrometer data processing: ten measurements were gathered by the spectrometer for each radiometric target, therefore ten spectral curves where obtained. The maximum and the minimum curves where filtered out and a curve resulting from the median values of the remaining curves was calculated.

The nominal reflectance values of the radiometric targets were compared to the values obtained by the spectrometer. In case the values were different, the reflectance measured by the spectrometer would be used in any further analyses involving target reflectance.

The spectral signature gathered for each reflectance target was reclassified, so that each wavelength would be assigned to the corresponding Ultracam multispectral band. Therefore the wavelengths between 400-600 nm were labelled as blue band (B), 480-600 nm as green band (G), 580-720 nm as red band (R), and 620-1000 nm as infrared band (IR). These threshold values were chosen as they are the minimum and maximum wavelengths for each Ultracam band, although it cannot be assumed that the spectral sensitivity of these bands are constant between the maximum and minimum values. The aim of this reclassification process was to be able to establish relationships between the data gathered by the spectrometer and the data registered by the camera for each spectral band.

The reflectance values measured for each pair of analogous reflectance targets were compared to see if each pair of targets could be considered as a unique target of 1 m x 2 m. Therefore the non-parametric Mann–Whitney U test for independent samples was conducted the reflectance values in bands B, G, R and NIR at a significance level of 5% ($\alpha = 0.05$).

Moreover, radiance was measured before and after the flight in Barakaldo, so the before and after values for each target were compared in order to check if the differences were significant. If the differences between the targets were not significant both measures could be used indistinctly in further analyses. The non-parametric Wilkoxon signed-rank test for two related samples was conducted for bands B, G, R and NIR at a significance level of 5% ($\alpha = 0.05$). If there were significant differences, the relationship between the radiance before and after the flight would be established, calculated by using the Spearman's rank correlation coefficient (Spearman's rho) at significance level of 5% ($\alpha = 0.05$) . This non-parametric test is a measure of statistical dependence which does not require a bivariate normal distribution for the data and therefore is more robust then the Pearson correlation coefficient.

2.1.4. Image calibration: the relationships between the data gathered by the camera (DNs) and the reflectance and radiance values measured by the spectrometer for the reflectance targets was established for each site in each orthophoto. The Spearman's rank correlation coefficients (Spearman's rho) at significance level of 5% ($\alpha = 0.05$) were also calculated for each site in each orthophoto.

3. RESULTS AND DISCUSSION

3.1 Ultracam X

Table 2 shows the descriptive statistics for each reflectance target according to the DN registered in the orthophoto 7018. The results of the DNs are shown for half of the targets. The sample size for each target was 36; none of the distributions fit a normal distribution according to the K-S test ($p>0.05$), therefore the use of non-parametric statistics (i.e. median) and tests was recommended. The same results were obtained for orthophoto 7016 and 7017.

Target	Statistic	Blue	Green	Red	NIR
BL_1	Mean	157.42	178.83	157.72	241.58
	Median	157.00	179.00	156.00	241.00
	SD	2.862	2.236	3.947	1.156
	Min	152	174	153	240
	Max	164	183	167	245
GR25_1	Mean	106.75	117.14	102.44	237.50
	Median	107.00	117.00	102.00	238.00
	SD	1.228	1.175	1.027	1.028
	Min	105	114	101	235
	Max	110	119	106	240
GR50_1	Mean	67.36	63.28	57.00	226.78
	Median	67.00	63.00	57.00	227.00
	SD	.931	.882	.676	1.290
	Min	65	61	56	224
	Max	69	65	58	229
GR75_1	Mean	35.44	25.00	25.14	206.33
	Median	35.00	25.00	25.00	206.00
	SD	1.027	.828	.899	2.293
	Min	34	24	24	202
	Max	39	27	28	214
NG_1	Mean	2.75	1.75	1.47	38.28
	Median	3.00	2.00	1.50	37.50
	SD	.500	.649	.560	3.369
	Min	2	1	0	33
	Max	4	3	2	44

Table 2. Descriptive statistics for orthophoto 7018.

The results of the Mann–Whitney U test comparing the DN registered by the camera for the targets with the same nominal reflectance showed that there were significant differences in all the bands (B, G, R, NIR) for all the grey targets (GR25, GR50 and GR75), in all the orthophotographs. Table 3 shows (in bold) the cases where there was no significant difference in the distribution (Sig. values greater than 0.05). They correspond to the black target (NG) in orthophotos 7016 and 7018, and the

NIR band for those targets in the orthophoto 7017. In addition, there were no significant differences between the white targets (BL) in the NIR in the orthophoto 7018.

	Target	BL	NG			
ID	Stat.	NIR	B	G	R	NIR
7016	U	243.00	618.00	637.50	640.50	590.50
	Z	-4.80	-0.39	-0.14	-0.10	-0.65
	Sig.	.000	**.695**	**.890**	**.922**	**.517**
7017	U	537.00	390.00	370.50	343.00	577.50
	Z	-1.32	-3.24	-3.69	-3.78	-0.80
	Sig.	.186	.001	.000	.000	**.425**
7018	U	529.00	613.00	602.50	621.50	407.00
	Z	-1.42	-0.48	-0.61	-0.34	-2.73
	Sig.	**.157**	**.631**	**.544**	**.732**	.006

Table 3. Results of the Mann–Whitney U test to compare targets (BL, NG) for different bands (B, G, R, NIR). U: Mann–Whitney U, Z: Z statistic, Sig.: bilateral asymptotic significance.

The Friedman test showed that the hypothesis that the DN for the same target in different orthophotographs could be rejected for all the targets when considering the B, G and R bands ($p<0.05$ in all cases), but not for the NIR band for all except three of the panels. Therefore the Wilkoxon signed-rank test was conducted for the NIR band for all the targets and compared the orthophotos in pairs; Table 4 shows the results for the targets where the distribution was not significant different ($\alpha = 0.05$) when comparing the NIR values between the orthophotos 7017 and 7018. In all the other cases and when they were compared to the values in the orthophoto 7016, the differences were significant.

	BL_1	BL_2	GR25_1	GR50_2	GR75_1	GR75_2	NG_2
Z	-1.42	-1.74	-1.40	-1.93	-1.26	-1.12	-1.18
Sig.	.153	.081	.161	.053	.206	.261	.236

Table 4. Results of the Wilkoxon signed-rank comparing the NIR band for the targets in orthophotos 7017 and 7018. Z: Z statistic, Sig.: bilateral asymptotic significance

The reflectance values obtained with the spectrometer for each of the targets were significantly different to the nominal reflectance, therefore the values obtained with the spectrometer were used as reference. The non-parametric Mann–Whitney U test to compare reflectance values for each pair of targets showed that the measured reflectance values were different for all the considered bands (visible and NIR), ($\alpha = 0.05$) but for the white targets (BL_1, BL_2) regarding the blue and green bands, as showed in Table 5.

Stat.	B	G	R	NIR
U	19609.00	15039.00	4482.00	13210.00
Z	-.508	-1.348	-7.972	-16.304
Sig.	**.612**	**.178**	.000	.000

Table 5. Results of the Mann–Whitney U test to compare the BL_1 and BL_2 targets' reflectance for different bands (B, G, R, NIR). U: Mann–Whitney U, Z: Z statistic, Sig.: bilateral asymptotic significance.

The results of the Mann–Whitney U test, which was used to compare the pairs of targets regarding the radiance values measured before and after the flight, showed that there were no significant differences ($\alpha = 0.05$) between each pair of targets for any of the four bands. This result was obtained for both the radiances measured before and after the flight. Table 6 shows the results for the comparison between the GR25 targets regarding the radiance values before the flight, as a sample of the results obtained for the rest of targets.

Stat.	B	G	R	NIR
U	176141.00	173881.00	174803.00	173189.00
Z	-.883	-1.376	-1.297	-1.299
Sig.	**.378**	**.169**	**.195**	**.194**

Table 6. Results of the Mann–Whitney U test to compare the GR25_1 and GR25_2 targets radiance measured before the flight for different bands (B, G, R, NIR). U: Mann–Whitney U, Z: Z statistic, Sig.: bilateral asymptotic significance.

The radiance values before and after the flight were compared using the Wilkoxon signed-rank test for each reflectance target. All the bilateral asymptotic significances were smaller than 0.05, therefore the radiances before and after the flight were different for any combination of band and target. Since the radiances were different, the Spearman's rank correlation coefficient (Spearman's rho) was calculated to establish the relationship between the radiances before and after the flight. Table 7 shows the Spearman's rho (r); all the correlations were significant at the 5% level.

		Radiance values before the flight				
	Bands		B	G	R	NIR
Radiance values after the flight	B	r	.952	.952	.952	.905
		Sig.	.000	.000	.000	.002
	G	r	.952	.952	.952	.905
		Sig.	.000	.000	.000	.002
	R	r	.952	.952	.952	.905
		Sig.	.000	.000	.000	.002
	NIR	r	.929	.929	.929	.881
		Sig.	.001	.001	.001	.004

Table 7. Correlations between the radiance values measured in the targets before and after the flight for different bands (B, G, R, NIR. r: Spearman's rho (r), Sig.: bilateral significance.

The Spearman's rank correlation coefficients calculated between the DNs (obtained from the orthophotos) and the radiance values were all greater than 0.95 and therefore significant at the 5% level, for each band in each of the three orthophotos. These results were obtained for the correlations with the radiance measured before the flight and for the correlations with the radiance measured after the flight. The correlations were better using the 10 radiometric targets than 8 targets (excluding GR50), and better than using 6 targets (excluding GR50 and GR75). The band most affected by the variation of the sample is the NIR, with a significant decrease in

the Spearman's rho. Table 8 shows the coefficient r for the correlations between the DNs and the reflectance using 10, 8 and 6 targets in one of the images (7098). The results for the other two orthophotos are analogous. In all cases all the correlations are significant at the 5% level and at the 1% level as well. These results indicate that there was a relationship between the at-surface reflectance and the DNs provided by the camera. This information, the DNs provided by the camera and at-surface reflectance, could be used to calibrate the image using an empirical line calibration.

Orthophoto 7098			Reflectance values			
		rho (r)	B	G	R	NIR
Digital Numbers (DNs)	10 targets	B	.978			
		G		.980		
		R			.977	
		NIR				.940
	8 targets	B	.958			
		G		.963		
		R			.956	
		NIR				.885
	6 targets	B	.949			
		G		.954		
		R			.945	
		NIR				.777

Table 8. Correlations between the reflectance and the DNs for different bands (B, G, R, NIR) in the orthophoto 7098. rho (r): Spearman's rho

3.2 Ultracam Xp

Table 9 shows the descriptive statistics for the reflectance targets according to the DNs registered in the orthophoto of Cogollos. The results are shown for half the targets per pair. The sample size for each target was 8, due to the larger GSD in comparison to the orthophotos from Barakaldo. The samples in this orthophoto did not fit the normal distribution ($p>0.05$ for the t-test).

Target	Statistic	Blue	Green	Red	NIR
BL_1	Mean	255.00	255.00	255.00	254.50
	Median	255.00	255.00	255.00	255.00
	SD	.000	.000	.000	.756
	Min	255	255	255	253
	Max	255	255	255	255
GR25_1	Mean	246.63	255.00	255.00	250.75
	Median	247.00	255.00	255.00	251.50
	SD	2.560	.000	.000	3.845
	Min	242	255	255	244
	Max	249	255	255	255
GR50_1	Mean	208.75	209.88	237.88	240.25
	Median	207.50	213.00	238.00	242.00
	SD	5.970	7.643	6.664	4.979
	Min	199	196	227	233
	Max	217	219	246	247
GR75_1	Mean	141.63	130.13	156.13	211.38
	Median	142.50	131.00	156.00	213.00
	SD	9.164	11.218	12.017	9.486
	Min	123	109	131	192
	Max	152	146	171	224
NG_1	Mean	14.50	.00	.00	71.50
	Median	14.00	.00	.00	66.50
	SD	5.398	.000	.000	11.174
	Min	8	0	0	62
	Max	21	0	0	89

Table 9. Descriptive statistics for the orthophoto from Cogollos.

The Mann–Whitney U test compared the ND corresponding to targets with the same nominal reflectance indicated that there were no significant differences (Sig. values greater than 0.05) for any of the compared pairs except for the targets with 50% and 0% nominal reflectance (for all the bands except the R and NIR in the 50% reflectance target) (Table 10). Nevertheless these results were obtained with a sample size of 16 points, which is less than the recommended minimum sample size (20) for the Mann-Whitney U test.

Target	Stat.	B	G	R	NIR
GR50	U	12.500	6.500	13.500	31.500
	Z	-2.059	-2.684	-1.954	-.053
	Sig.	.040	.007	**.051**	**.958**
NG	U	9.000	12.000	12.000	10.500
	Z	-2.424	-2.554	-2.554	-2.265
	Sig.	.015	.011	.011	.024

Table 10. Results of the Mann–Whitney U test to compare targets (GR50, NG) for the different bands (B, G, R, NIR). U: Mann–Whitney U, Z: Z statistic, Sig.: bilateral asymptotic significance.

As for the data set A, the reflectance values obtained with the spectrometer for each of the targets were significantly different to the nominal reflectance; therefore, the values obtained with the spectrometer were used as reference. The non-parametric Mann–Whitney U test was used to compare the reflectance values for each pair of targets showed that the measured reflectance values were different for all the bands ($\alpha = 0.05$) except for the black and GR75 targets regarding the visible bands (Table 11).

Target	Stat.	B	G	R	NIR
GR75	U	19906.00	15889.00	8823.00	28969.00
	Z	-.253	-.494	-1.632	-9.597
	Sig.	**.800**	**.622**	**.103**	.000
NG	U	19192.00	15458.00	4387.00	16004.00
	Z	-.866	-.927	-8.110	-15.115
	Sig.	**.387**	**.354**	.000	.000

Table 11. Results of the Mann–Whitney U test to compare the GR75 and NG targets' reflectance for the different bands (B, G, R, NIR). U: Mann–Whitney U, Z: Z statistic, Sig.: bilateral asymptotic significance.

Table 12 shows the Spearman's rank coefficients for the correlations between DNs and the reflectance values measured on the targets. The reflectance values for the BL_2 target were excluded, since the BL_2 target was an outlier, since its reflectance was smaller than the reflectance of all the other targets except for the black ones. All the correlations were significant at the 5% level and at the 1% level, and the best results were obtained correlating data from 9 targets instead of 7 (which meant excluding the GR50 targets). As for the data set A, the most sensitive band to these changes within the sample was the NIR. In the same way, the existence of a relationship between the at-surface reflectance and the DNs provided by the camera suggests the possibility of using an empirical line calibration to obtain an at-surface reflectance image.

			Reflectance values			
		rho (r)	B	G	R	NIR
Digital Numbers (DNs)	9 targets	B	.964			
		G		.967		
		R			.962	
		NIR				.917
	7 targets	B	.933			
		G		.936		
		R			.927	
		NIR				.863

Table 12. Correlations between reflectance and DN for different bands (B, G, R, NIR) and different target sets. rho (r): Spearman's rho

3.3 GSD influence in the calibration process

The maximum number of pixels which could be identified in each calibration target in set B was small. Moreover, it was very difficult to find homogenous pixels. These two aspects regarding the sample characteristics, made it difficult to conduct reliable statistical analyses. Thus, the calibration of images with a GSD of 25 cm (set B) would be more reliable using calibration targets larger than 1 m x 1 m,

Part of the success of the calibration process using an empirical line calibration to obtain at-surface reflectance depends on the correlation between the DNs and the reflectance measurements in the targets. Therefore, if the pixels cannot be identified properly on the targets and/or the pixel does not correspond exclusively to the target, the regression output might not be satisfactory. This aspect can be noted by comparing the correlation coefficients for the DNs and the reflectance values for both data sets. Looking at table Table 8 and Table 12 it can be seen that the data set A (GDS = 7 cm) obtained better results than the data set B (GDS = 25 cm). The results for data set A were better than the results for data set B for all three orthophotos.

3.4 Suitability of the calibration for the imagery gathered by the National Plan of Aerial Orthophotography (PNOA).

Nowadays the images gathered by the PNOA have a GSD of 25 cm or 50 cm, which would require larger calibration targets to perform a successful at-surface reflectance correction using an empirical line calibration approach, as discussed above. Nevertheless, the high correlation coefficients between the DNs and the at-surface reflectance values suggest that it can be satisfactory.

It has been shown that three consecutive images gathered with the same camera, during the same flight, and under very similar conditions (data set A) had significant differences in the DNs for the same targets. This means that each image would need a different equation to be radiometrically corrected. In addition, using level 2 imagery instead of level 3 imagery is recommended, so that the original DNs are kept.

Odi (2009) conducted similar research for images gathered by the DMC camera for the PNOA in Castilla-La Mancha (SE Spain), considering the bidirectional reflectance distribution functions in their approach. The preliminary results showed that the radiometric corrections improved the quality of the images.

Qualitative classifications can be performed once the images are radiometrically corrected (e.g. relative correction); although to estimate biophysical variables (i.e. biomass) the estimation of the at-surface reflectance is a required step.

REFERENCES

Cramer, M., 2005. Digital airborne cameras — status and future. Proceedings of ISPRS Hannover Workshop 2005: High-Resolution Earth Imaging for Geospatial Information. 8 p., on CD-ROM.

Markelin, L., Honkavaara, E., Peltoniemi, J., Ahokas, E., Kuittinen, R., Hyyppä, J., Suomalainen, J., Kukko, A., 2008. Radiometric calibration and characterization of large-format digital photogrammetric sensors in a test field. *Photogramm. Eng. Remote Sens*. 74, pp. 1487-1500

Honkavaara, E., 2004. In-flight camera calibration for direct georeferencing. In: *International Archives of Photogrammetry, Remote Sensing and Spatial Information Sciences*, 35, Part B1, pp. 166–171

Honkavaara E., Arbiol R., Markelin L., Martinez L., Cramer M., Bovet S., Chandelier L., Ilves R., Klonus S., Marshal P., Schläpfer D., Tabor M., Thom C., Veje N., 2009. Digital Airborne Photogrammetry—A New Tool for Quantitative Remote Sensing?—A State-of-the-Art Review On Radiometric Aspects of Digital Photogrammetric Images. *Remote Sensing*, 1(3), pp. 577-605

Odi M., 2009. Experiencias en radiometría de campo. In: *Seminario en avances de espectro-radiometría,* CCHS-CSIC, pp. 45-48.

ACKNOWLEDGEMENTS

This research has been partially funded by the Junta de Castilla y León through the project "Calibración radiométrica de cámaras aéreas digitales. Aplicación a la clasificación automática de cubiertas del suelo y estimación de biomasa" (LE001B08).

This research has been developed in collaboration with WIDE WORLD GEOGRAPHIC, S.L. within the project "Calibración radiométrica de imágenes digitales para el control de cambio climático y biomasa en áreas contaminadas o degradadas mediante empleo de la banda infrarroja".

The authors would like to thank Javier Núñez Llamas for all the assistance during the field work and Lucas Martínez for his comments.

The authors would like to thank Bonsai Advanced Technologies for their assistance concerning the use of the spectrometer.